The Canadian Mineralogist
Vol. 33, pp. 293-302 (1995)

PIXE ANALYSIS IN MINERALOGY AND GEOCHEMISTRY

NORMAN M. HALDEN

Department of Geological Sciences, University of Manitoba, Winnipeg, Manitoba R3T 2N2

JOHN L. CAMPBELL AND WILLIAM J. TEESDALE

Department of Physics, University of Guelph, Guelph, Ontario N1G 2W1

ABSTRACT

Proton-induced X-ray emission can be used to analyze geological samples for a wide range of trace elements (including transition, large-ion-lithophile and high-field-strength elements, and, in favorable circumstances, rare-earth elements) in a variety of minerals down to levels of a few parts per million. The analyses are simultaneous, multi-element, and nondestructive. A focused beam of protons (spot sizes typically 5 × 5 μm) can be used for point analyses, or the beam may be scanned over an area as large as 2 mm × 2 mm to provide a two-dimensional X-ray map of element distribution. The proton beam also may be used for nuclear reaction analysis and proton-induced gamma-ray emission. These techniques may be run concurrently with PIXE and are useful for analyzing a sample for light elements such as Li, B and F, with detection limits in the region of 100 ppm.

Keywords: proton-induced X-ray emission, microprobe, trace elements.

SOMMAIRE

L'émission de rayons X due à un faisceau de protons (PIXE) peut servir à analyser des échantillons géologiques pour tout un éventail d'éléments traces, y inclus les éléments de transition, les éléments lithophiles à large rayon, les éléments à large rapport de charge à rayon ionique, et même, dans certaines conditions favorables, les terres rares; cette technique vise une grande variété de minéraux, et les seuils de détection sont de quelques parties par million. Les analyses pour plusieurs éléments sont simultanées, et non destructives. Un faisceau de protons ayant un foyer de 5 × 5 μm, typiquement, peut mener à une analyse ponctuelle; par contre, le faisceau peut aussi balayer une surface mesurant jusqu'à 2 mm × 2 mm pour produire une carte de distribution des éléments en deux dimensions à partir des intensités de rayons X repérées. On peut aussi utiliser le faisceau de protons pour l'analyse d'une réaction nucléaire et d'émissions de rayons γ produits, et ceci en même temps que se poursuit l'analyse PIXE. Ce développement permet l'analyse des échantillons pour leur teneur en Li, B et F, avec un seuil de détection d'environ 100 ppm.

(Traduit par la Rédaction)

Mots-clés: émission de rayons X induite par protons, microsonde, éléments traces.

INTRODUCTION

The application of Proton-Induced X-ray Emission (PIXE) to geological problems began in the mid-1970s; one of the first studies was that of Horowitz & Grodzins (1975) on sphalerite. Since then, PIXE has seen increasing application to a variety of geological problems as data-reduction techniques have improved, a microprobe capability has been developed (micro-PIXE), and Scanning Proton Microprobes (SPM) have begun to provide two-dimensional X-ray images of minor- and trace-element distributions in minerals (Teesdale *et al.* 1993). Although PIXE provides some exciting new insights into the trace-element chemistry of minerals, its use has been somewhat restricted because it requires a particle accelerator, and is currently available only in a few laboratories.

By the late 1980s, two variants of PIXE had been developed. The first, which is the more widely used, is based on a small electrostatic accelerator and operates in the 2–4 MeV range of proton energy (Johansson & Campbell 1988). The second type, a high-energy variant of PIXE, is based upon a cyclotron accelerator that produces protons in the 40–60 MeV range. Halden *et al.* (1991) and Peisach & Pineda (1990) showed that *K* X-rays of geologically important trace elements

(Z > 50) can be generated, including those of the rare-earth elements (*REE*), large-ion-lithophile (*LIL*) elements, and precious-metal elements. Durocher *et al.* (1988) suggested that analysis with high-energy protons has the potential to alleviate the problem of spectral overlap among *K* and *L* X-ray lines, which is a common occurrence in the 5–20 keV X-ray energy region with conventional PIXE. However, high-energy PIXE has not evolved to the level of technology or data-handling currently available in conventional PIXE; its detection limits, although theoretically in the high ppb range for the *REE*, have never been demonstrated in practical microprobe analysis of minerals.

Early reviews of the uses of PIXE were written from a physics perspective (Cahill 1980, Rogers *et al.* 1984) because the work was focused primarily on the technology, and because software for data processing was at the development stage. More recently, review papers (*e.g.*, Annegarn & Bauman 1990, MacArthur & Ma 1991) and papers on the comparison of techniques (*e.g.*, Campbell *et al.* 1990) have taken on a geological flavor because there are more and more problems that require micro-analytical techniques for trace-element analysis of minerals. Fraser (1990) provided an overview of the uses of the scanning proton microprobe, and Reed (1990) included PIXE in his review of micro-analytical techniques.

PIXE is now a mature analytical technique that is seeing application in an increasing variety of mineralogical and geochemical problems (Czamanske *et al.* 1993). PIXE also has been used to analyze such materials as lake sediments (Palmer *et al.* 1989, Grime & Davison 1993). Campbell *et al.* (1995) describe many of the technical details of PIXE analysis. From the geological perspective, the key point is that PIXE is the direct proton analogue of the electron microprobe; for anyone familiar with energy-dispersion electron-microprobe analysis (EPMA), the transition to PIXE analysis is straightforward.

EARLY PIXE

Early PIXE studies (*e.g.*, Horowitz & Grodzins 1975) were done with a pin-hole-collimated proton beam; this experimental arrangement is very different from present-day quadrupole-magnet focussing systems that have the capability of providing beams of less than one micrometer across. The 1970s were the time of the Apollo missions, and lunar samples were the source of many interesting studies. Blank *et al.* (1984) studied the partitioning of Zr and Nb among ulvöspinel, chromite, ilmenite and armalcolite in order to determine the cooling history of samples from a variety of Apollo landing sites. In these minerals, Zr is present in the 70–500 ppm range, and Nb, in the 10–30 ppm range. Perhaps more important from a petrogenetic viewpoint was the observation that the compositions varied within exsolution lamellae and at the margins of grains, thereby indicating that trace elements were distributed heterogeneously on a small scale. Environmental concern about coal-fired generating stations promoted a number of detailed studies of the composition of coal. Coal can contain a variety of trace elements that are heterogeneously distributed on a small scale; furthermore, these elements are liberated to the atmosphere on burning. Coal is particularly amenable to PIXE analysis because with carbon as the main constituent, the matrix presents few matrix-correction problems. Chen *et al.* (1981) and Valkovič *et al.* (1984) showed that coal contains a host of trace elements whose concentrations vary among the different types of coal macerals; elements such as Zn, As, Se and U were detected down to the 10 ppm level.

Lucas *et al.* (1981) attempted to date zircon crystals from the Amitsoq gneiss, Greenland, by determining their U, Pb and Th contents using PIXE. However, in the absence of isotopic analysis, these were at best "model ages" and would not be considered geologically significant in the context of our current knowledge of isotope systematics. It may be possible to do isotopic analysis using high-energy protons. However, it is unlikely that proton activation analysis (PAA) will have sufficient sensitivity for geochronological applications.

QUANTITATIVE ANALYSIS BY MICRO-PIXE

One of the main reasons why PIXE is a sensitive analytical technique is the inherently low continuous background-radiation emitted during deceleration of protons in the sample. Relative to characteristic X-ray signals from elements in the specimen, the corresponding *bremsstrahlung* background in EPMA is much more intense (Kullerud *et al.* 1979). In the early stages of PIXE development, there was an anticipation of extremely low detection-limits, but it was soon realized that secondary *bremsstrahlung* emitted by electrons set in motion by the primary protons would be the determining factor for limits of detection. Therefore, PIXE is *not* an ultra-trace analytical technique like mass spectrometry or neutron-activation analysis (Cahill 1980). Rather, it is a nondestructive multi-element microprobe technique capable of detection limits down to the ppm level.

The basic elements of automated and quantitative PIXE are described by Campbell & Cookson (1984), Maxwell *et al.* (1984, 1989) and Ryan *et al.* (1990). A mathematical model of the spectrum is fitted to the observed spectrum and optimized using the chi-squared criterion, and relative peak-intensities are derived (Maxwell *et al.* 1984). The objective is to convert the measured X-ray yields into concentrations of elements (more details are provided in Campbell *et al.* 1995). Campbell *et al.* (1986) used this approach to calibrate micro-PIXE analysis of sulfide minerals in a comparative study of two proton microprobes using a pyrrhotite standard containing trace Pd and Se; they showed that accuracy of better than ±10% relative can be achieved for elements down to $Z = 30$.

Accuracy, precision and minimum detection limits of PIXE analyses are described in detail by Campbell *et al.* (1988), and with specific reference to well-characterized minerals and glasses, by Czamanske *et al.* (1993). With a 3 MeV proton beam, and beam currents of 10–15 nA and a duration of analyses of 3–4 minutes, detection limits for Ni, Cu, Zn, Ga, Rb, Sr, Y, Zr, Nb and Ba were found to range from 2 to 50 ppm in a glass prepared from USGS standard BHVO–1; relative accuracy ranged from –15% for Rb to +18% for Cu; precision, expressed as deviation in relative % from the mean value of five replicate measurements, ranged from as low as 1% for Sr to 24% for Ba (see Table 1 in Czamanske *et al.* 1993). Detection limits, which are a function of the charge used (and therefore the total accumulated counts) can be lowered using longer count-times. Defocussing the beam in such circumstances may be required to minimize overheating of the sample.

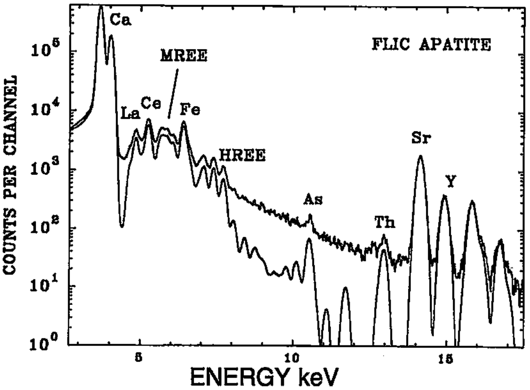

FIG. 1. PIXE spectrum of apatite from the Falcon Lake igneous complex. The raw data are shown in the upper spectrum; the lower line is the fitted spectrum with the background removed. The *K* X-ray lines of Ca, Fe, As, Sr and Y and the *L* X-ray lines of *REE* and Th are visible. Detection limits for Sr and Y are typically about 5 ppm in apatite, for the light *REE*, about 100 ppm, for the heavy *REE*, 40 ppm, and for Th, about 20 ppm.

Analysis of Accessory Minerals

Accessory minerals are the principal hosts for the high-field-strength elements (*HFSE*), rare-earth elements (*REE*), and large-ion lithophile (*LIL*) elements. Many petrogenetic models of fractional crystallization and partial melting hinge on knowledge of the partition coefficients of such trace elements among minerals. Recent work has shown that many accessory minerals are zoned, and that at least some of this zoning involves trace-element variation decoupled from that of major elements, a phenomenon that can occur on very small scales (*e.g.*, Shimizu 1990, Halden *et al.* 1993). The combination of PIXE and SPM can provide both trace-element concentrations and a map of trace-element distribution.

Apatite

Rogers *et al.* (1984) analyzed apatite from Durango, Mexico; their PIXE results show good correspondence with XRF results. *REE* contents were found to range from <17 ppm for Er to 4400 ppm for Ce; the apatite contains less than 15 ppm U and between 230 and 480 ppm Th, Y and Sr. Roeder *et al.* (1987) reported a more extensive study of the abundance of *REE* in apatite, including some samples from Durango; the results obtained using PIXE were found to be similar to those obtained by Rogers *et al.* (1984). Apatite is a very suitable mineral for PIXE analysis because the X-ray lines of the principal major elements, Ca and P, do not interfere with those of the trace elements. Figure 1 shows a typical spectrum collected from apatite; the apatite crystal is zoned and is from part of an apatite-rich layer in the Falcon Lake igneous complex, Manitoba (Mandziuk *et al.* 1989). The X rays of the transition elements, the *HFSE*, As, Rb and Sr are easily resolved, with detection limits in the 2–10 ppm range. For the *REE*, the situation is more complicated because the *L* X-rays for the *REE* occur in the 4.6–9 keV region. There is considerable spectral overlap because of the geochemical coherence of the *REE*, and because each *REE* emits several *L* X-ray lines. Nonetheless, useful data may be obtained for the *REE*, with detection limits in the 17–50 ppm range; this is sufficient to characterize between the compositions of oscillatory zones where they are encountered in apatite.

Zircon

As in the case of apatite, the X-ray lines of many of the trace elements of interest in zircon do not overlap major elements (Zr and Hf) in a PIXE spectrum. Figure 2 shows a typical spectrum collected from zircon, and Table 1 shows quantitative trace-element data derived from such a spectrum. The low-energy tail of the very intense Zr*K*α line obscures the Y*K*α line, making Y determination difficult. This effect arises from Compton scattering (into the detector) of the Zr X-rays that were originally directed elsewhere. Fitting of this type of overlap requires deconvolution of the spectrum of pure zirconium to determine the correct

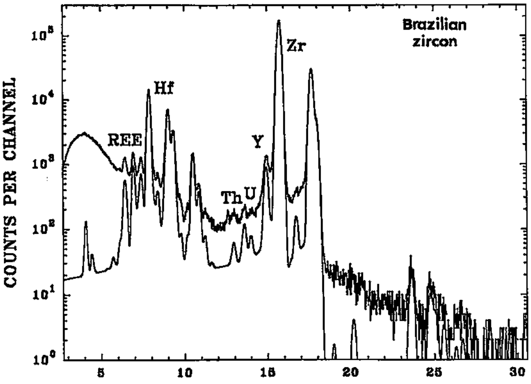

FIG. 2. PIXE spectrum of zircon from Novo Horizonte in Brazil, showing the *K* X-ray lines of Zr and Y and the *L* X-ray lines of the REE, Hf, Th and U. The data in Table 2 were derived from this and similar spectra (Halden *et al.* 1993).

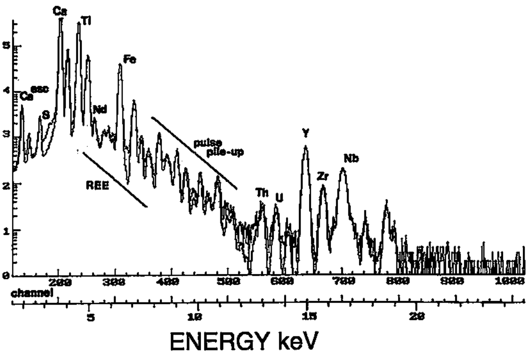

FIG. 3. PIXE spectrum of Cardiff titanite. Ca, Ti and Fe *K* X-ray lines and pulse-pile-up peaks obscure the 4 to 11 keV region of the spectrum. Notwithstanding this, it is still possible to resolve the Nd $K\alpha$ X-ray line at 4.95 keV. In the 12 to 20 keV region, it is possible to resolve the *K* X-ray lines of Y, Zr and Nb and the *L* X-ray lines of Th and U. Table 2 gives quantitative data and detection limits.

line-shape for the Zr$K\alpha$ X-rays, including the low-energy feature that overlaps any Y$K\alpha$ X-ray line present. The net result of this problem is that the detection limit for Y in zircon is about 200 ppm (Halden *et al.* 1993). In this energy region of the spectrum, this problem will occur where X rays generated by trace elements occur in the presence of X rays of slightly higher energy generated by major elements; examples include trace Rb, Sr and Zr in the presence of major Sr, Zr and Nb, respectively. Notwithstanding the difficulties encountered in processing the Y peak, the PIXE data in Table 1 show the difference in chemistry between the core and the overgrowth, particularly with regard to levels of Y and Yb.

TABLE 1. MICRO–PIXE DATA FOR TRACE ELEMENTS (ppm) IN A ZONED CRYSTAL OF ZIRCON FROM NOVO HORIZONTE, BRAZIL

	core	3	2	3	7	8	9	og	1σ	LOD
Zr	54.8	51.1	51.9	51.1	54.5	50.7	51.2	50.6	0.04	0.01
Hf	8200	7640	7900	7560	8570	7870	8050	8050	38	138
Zr/Hf	65.8	66.9	65.7	67.7	63.6	64.4	63.7	62.9		
Fe	213	76	48	38	231	130	239	—	4	8
Y	2498	2235	1974	1822	2814	2235	2122	311	37	100
Gd	131	—	—	—	129	—	—	—	12	25
Dy	312	213	182	164	307	224	201	—	17	36
Er	339	286	210	210	338	258	245	—	16	38
Yb	486	487	452	393	497	395	309	84	13	24
ΣREE	1286	986	844	767	1271	877	7555	84		
Th	1517	362	362	261	1973	978	723	—	30	46
U	1092	582	419	430	1304	761	714	—	33	52

The concentration of Zr is given in wt%. Analyses 1–9 correspond to luminescent zones shown in Halden *et al.* (1993, Fig. 5). LOD: average lower limit of detection, expressed in ppm. ——: concentration is below LOD + 3σ; 1σ average error die to spectrum fitting; og: overgrowth.

Titanite

The analysis of titanite illustrates the problem of trace-element X-ray lines being obscured by those emitted by major elements constituting the mineral. In this case, *K* X-ray lines from Ti, Mn and Fe obscure *L* X-ray lines from the *REE* (Fig. 3). Careful fitting of the

TABLE 2. TRACE–ELEMENT DATA (ppm) FOR THE CARDIFF TITANITE, AS OBTAINED BY PIXE

	004	σ	LOD	005	σ	LOD	006	σ	LOD
Sr	65	15	16	85	15	19	71	16	23
Y	6631	100	58	6688	100	59	6836	101	67
Zr	1182	55	74	1122	55	82	1124	54	67
Nb	2991	124	234	3358	129	241	3174	125	235
La	——	——	——	4044	3285	3429	3656	3260	3393
Ce	5344	1087	2240	5922	1080	2238	5697	1074	2225
Nd	2896	142	321	2829	151	344	2920	145	330
Sm	824	93	220	868	96	233	939	95	228
Gd	309	91	206	393	92	210	391	92	209
Er	1106	227	467	1218	227	465	1249	228	467
Yb	740	70	178	665	71	182	843	73	189
Lu	280	56	172	311	58	127	358	59	125
Hf	120	48	98	207	49	101	172	51	103
Th	513	55	56	579	54	47	562	54	58
U	689	56	43	434	56	45	564	55	57

1σ: standard deviation related to the spectrum–fitting procedure. LOD: typical lower limits of detection, in ppm. ——: concentration is below LOD + 3σ. The crystal of titanite (sample M28696) was obtained from the Department of Mineralogy, Royal Ontario Museum, Toronto. It is black and "glassy", and was collected from the Cardiff uranium mine, Ontario.

spectra and well-determined absorption corrections are necessary to extract worthwhile information. Note, however, that the X-ray lines of U, Th, Y, Zr, Nb and Sr occur in clear regions of the titanite spectrum; therefore, detection limits for these elements may be in the 5–20 ppm range (Table 2). In the case of apatite and titanite, some high-energy PIXE spectra illustrate that it is possible to resolve *K* X-rays of the *REE* in the 40–60 keV region, well-removed from any overlap problems due to constituent major elements (Durocher *et al.* 1988, Halden 1993).

Carbonate minerals

From a microbeam perspective, carbonate minerals present physical problems, as they are susceptible to ablation damage. In EPMA, beam conditions of 20–40 kV and 10 nA (typical for the analysis of silicate minerals for trace elements) produce ablation in the sample after about 10 seconds of exposure. During ablation, count rates from various elements (such as Na and Ca) decrease, leaving insufficient time to collect meaningful trace-element data. The main problem here is that the reduction in count rates for major elements will lead to erroneous matrix-corrections for trace and minor elements. There is also the potential for diffusion of elements away from the beam. As part of an exhaustive study of electron-microprobe effects on fish otoliths (which consist of calcite), Gunn *et al.* (1992) examined some of these problems. Some of the interest lies in the variability of the Sr/Ca ratio in growth zones observed in otoliths, as this ratio may be related to the temperature of the water inhabited by the fish. Sr levels are typically well below ~500 ppm, levels difficult to measure well by EPMA.

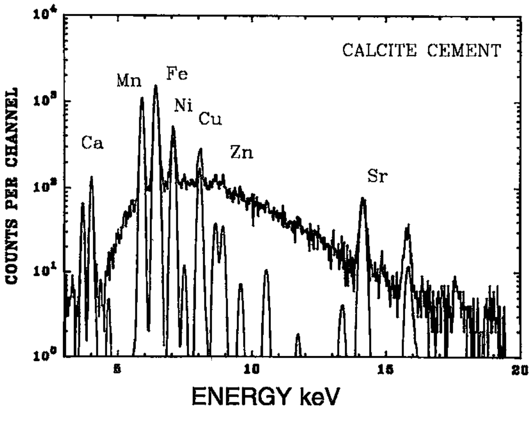

FIG. 4. PIXE spectrum of calcite from a diagenetic cement in the Elm Point Formation, in Manitoba. The *K* lines of Ca are filtered to reduce the total counts in the spectrum due to Ca. The *K* X-ray lines of Mn, Fe, Ni, Cu, Zn and Sr can be resolved; Table 3 gives quantitative data from dolomite and calcite from a variety of sources.

TABLE 3. TRACE-ELEMENT DATA (ppm) FOR SELECTED SAMPLES OF CARBONATES

	1	2	3	4	5	6	7	8	9	10	1σ[1]	LOD
Mn	103	838	153	156	64	15	70	85	–	–	8	14
Fe	84	546	569	953	477	290	708	946	16	13	9	12
Cu	–	32	–	–	–	14	14	12	21	11	2	3
Zn	–	6	17	7	9	11	9	8	16	9	2	2
Sr	51	37	101	77	520	239	151	151	669	1560	3	2

Analyses 1–4: calcite cements from the Elm Point Formation, Manitoba; 5–6: brachiopod fragments from the Elm Point Formation; 7–8: dolomite from the Elm Point Formation; 9–10: calcite otolith from a (Recent/extinct) Atlantic cod. [1] Typical 1σ statistical error (in ppm) from the spectrum–fitting procedure. LOD: typical lower limits of detection, in ppm.

Fraser *et al.* (1989) have shown that a combination of PIXE analysis and scanning proton microprobe mapping can be used to image trace-element variations in dolomite. Wogelius *et al.* (1992) used PIXE to analyze calcite and dolomite cements for their trace elements, the data being used to estimate the trace-element contents of the waters from which the cements were precipitated. A typical PIXE spectrum collected from calcite (Fig. 4) shows well-resolved *K* X-ray lines for Mn, Fe, Cu, Zn and Sr. Table 3 shows some trace-element concentrations derived from PIXE spectra of carbonates; in all cases, the detection limits are in the 2–15 ppm range. Sections containing carbonate minerals should be at least 40 μm thick, as the depth from which more than 90% of the X-ray yield originates (for most trace elements of interest in carbonates) is approximately 40 μm (see Campbell *et al.* 1995). If the proton beam penetrates to the mounting medium or glass slide, extraneous X-rays will be present in the spectrum.

PIXE can also be used to analyze carbonates for the rare earths without sample ablation. Figure 5 shows an SPM two-dimensional X-ray map and a line scan of a crystal of synthetic calcite doped with Tb; the Tb shows a zonal distribution. The calcite crystal was synthesized with a nominal bulk concentration of 746 ppm Tb. Analysis of the high-Tb and low-Tb regions on the line-scan shows that their respective Tb concentrations (~1400 and ~520 ppm; detection limit 25 ppm) straddle the nominal value.

PETROLOGICAL STUDIES

Mineral deposits

Cabri (1988) has reviewed the application of PIXE to ore-deposit studies, and also has provided much useful guidance on the preparation of samples for analysis. PIXE excites X rays from the top 20 μm of material in sulfide minerals, and particular care has to be taken in selecting points for analysis with reflected-light microscopy. In a study of ore materials from Kidd

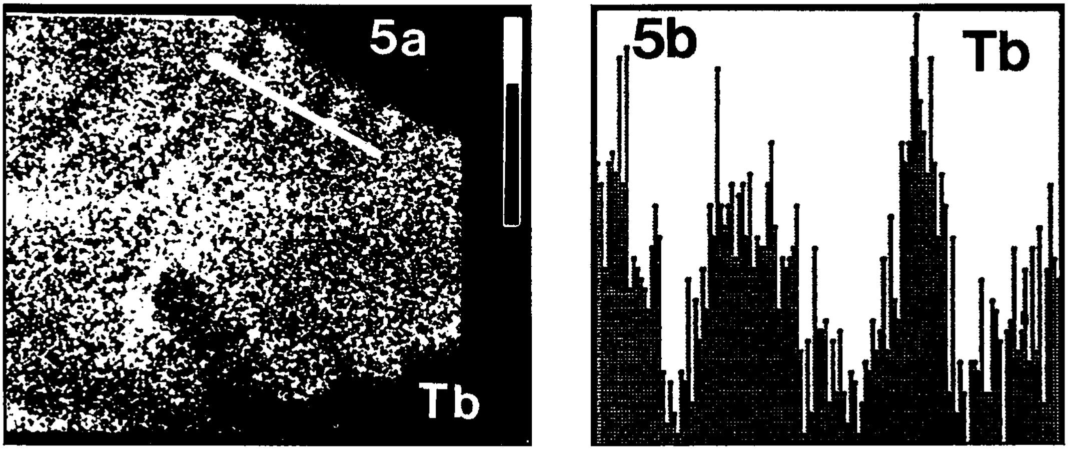

FIG. 5. Scanning proton microprobe (SPM). Two-D element map and line scan of Tb distribution in synthetic calcite. In the element-distribution map (a), light regions represent areas of high Tb content, and dark regions represent regions of low Tb content. The line on the map corresponds to the position of the line scan (b). Point analyses in the regions of high and low concentration show ~1400 ppm and ~520 ppm Tb, respectively (limit of detection, 25 ppm; 1σ fitting errors *ca.* 20 ppm); the nominal bulk composition is 746 ppm.

Creek, Geco and Mattagami–Norita, Cabri *et al.* (1985) showed that sulfide minerals could be analyzed for Ge, As, Se, Ag, Cd, In, Sn and Sb with detection limits of 7–20 ppm. The *K* X-rays for these elements have energies in excess of 10 keV, and their lines are free of interference from S and Fe X-rays. PIXE detection limits for many elements in sulfide minerals are in the 5–30 ppm range (~5 ppm for Ag, Pd and Rh, and ~20–30 ppm for Pt and Au using *L* X-rays).

Pyrite is a ubiquitous sulfide mineral associated with Au mineralization. Poor recovery of Au from pyritic ores has led to the suspicion that trace Au may be structurally bound within pyrite as so-called "invisible" gold. Analysis of pyrite for Au appears to be an appropriate application for PIXE; the *K* X-rays of Fe and S are well removed in energy from the 9.7 keV $L\alpha$ line of Au. However, the presence of As (10.54 keV $K\alpha$ X-ray) in such situations effectively precludes the analysis of pyrite for Au in the low-ppm range (in anything but ideal circumstances) because of spectral overlap. Campbell *et al.* (1988) found that under favorable conditions, detection limits for Au are in the 20–30 ppm range, depending upon the matrix. Griffin *et al.* (1991) quoted similar limits of detection in their study of pyrite from a Ag–Au deposit.

Czamanske *et al.* (1992) used PIXE to analyze major coexisting Cu–Fe–Ni sulfide minerals in Cu–Ni–PGE ores from the Noril'sk–Talnakh region of Siberia for trace elements from Co to Bi. The reported limits of detection for elements from Zn to Bi were found to range from 4 to 50 ppm. This work showed that it is possible to analyze chalcopyrite, cubanite and mackinawite for Pd in the 7 to 3000 ppm range; on the other hand, Pt, Ru and Rh were rarely found at levels above their minimum limits of detection in any of the minerals analyzed (4–5 ppm for Rh and Ru; 18–45 ppm for Pt). Czamanske *et al.* (1992) showed that (1) Pd concentrations in pentlandite are related to ore type and not to $f(S_2)$, the Ni/Fe ratio of pentlandite, or bulk Pd concentration, and (2) Se is uniformly distributed among the sulfides.

With regard to sulfide minerals, a combination of EPMA, back-scattered electron imaging and PIXE also may be used to improve techniques of ore beneficiation and mineral processing. It is important to know which mineral(s) contain such trace elements as Se, As and Cd because these elements are biologically active. If they are concentrated in a particular phase, or are associated with a particular type of ore, ore processing may be designed to minimize their environmental impact in tailings ponds (*cf.* Cabri *et al.* 1985). With the advent of the scanning proton microprobe, two-dimensional X-ray maps of trace-element distribution can be used in a manner similar to current practice for major elements with EPMA and image analysis; such studies have been aimed at improving the efficiency of ore beneficiation (Petruk 1989).

Mantle petrology

A number of elements, (*e.g.*, Rb, Y, Zr, Nb, Sr and the *REE*) can show open-system behavior in mantle rocks, and mobility of these elements has been linked to mantle metasomatism. A better knowledge of the partitioning of these elements and how they migrate will improve our understanding of mantle dynamics (*cf.* Adam *et al.* 1993; Green *et al.* 1989). Micro-PIXE provides an interesting insight into mantle processes, particularly where used in conjunction with the scanning proton microprobe. Early work (Fraser *et al.* 1984) showed that Sr could be concentrated at grain boundaries in garnet lherzolite, the inference being that grain boundaries acted as conduits along which elements could migrate. On the other hand, O'Reilly *et al.* (1991) used micro-PIXE to determine the distribution of trace elements in spinel lherzolite; they concluded that the trace elements are concentrated in "acceptor" minerals, such as phlogopite and apatite, and that trace elements do not occur in appreciable amounts at grain boundaries. Direct determination of trace-element concentrations at grain boundaries is limited because PIXE software models a homogeneous distribution of trace elements throughout the analytical volume sampled by the proton beam. There are few studies of element distribution at mineral surfaces, and much more work could be done in this area by making effective use of SPM and PIXE.

Micro-PIXE analysis of minerals from kimberlite and lamproite inclusions has been used to assist in diamond exploration. Griffin *et al.* (1988) analyzed a variety of minerals from eclogite from the Argyle field in Australia. Partitioning of Sr, Ga and Zr between garnet and clinopyroxene occluded in diamond was shown to be temperature-dependent. Variation in trace-element content of inclusions may be attributed to (1) open-system behavior, as the diamond crystals grew over an extended range of temperature and entrained a variety of inclusions, or (2) rapid growth that precluded equilibrium partitioning of trace elements in inclusions. In an extension of this work (Griffin *et al.* 1990), Ni partitioning between Cr-rich pyrope and olivine was shown to be related to temperature. This relationship has made it possible to characterize kimberlites with respect to the depth and temperature of their source region, and thus with respect to their diamond potential.

DISCUSSION

User-friendly PIXE

The restriction of PIXE to particle accelerators has, in the past, left Earth scientists unaware of the potential of this type of analysis for mineralogical and petrological problems. In the early days, analyses were computationally intensive, and the results of questionable quality. Even though the concentrations of trace elements could be measured with low detection-limits, this was insufficient to attract geologists, as it seemed that mass spectrometry and neutron activation could provide even lower detection-limits. As trace-element analysis has become increasingly routine, it has become apparent that trace-element partitioning, distribution and concentration are more heterogeneous than was previously realized. Microbeam analytical techniques are necessary to address problems of micrometer-scale mineral zoning. Rather than being seen as a complicating factor in analysis, such heterogeneity and zoning can be viewed as providing new insight into mineral growth.

As Earth scientists have come to view micro-PIXE as the proton analogue of EPMA, inhibitions have diminished. A major contributory factor in this has been the construction of target chambers dedicated to mineral analysis, chambers that incorporate many of the characteristics of the electron microprobe (Perujo *et al.* 1988). Cabri (1988) also has described the need for rapid data-processing, and for well-characterized absorbers and standards. The strengths of micro-PIXE derive from (1) its ability to analyze minerals using existing methods of sample preparation, (2) the nondestructive nature of the technique, (3) the simultaneous and multi-element nature of the analysis, and (4) the option of concurrent one-dimensional and two-dimensional imaging by scanning proton microprobe. Pitfalls in micro-PIXE analysis of minerals derive from (1) spectral overlap from geochemically coherent elements, and (2) the depth of penetration of the proton beam. Prior mineralogical and geochemical characterization of a mineral, together with effective spectrum-reduction procedures, can minimize problems related to spectral overlap. Of course, the expectation that PIXE can solve *all* multi-element analytical problems is unrealistic; no technique can do this. Good optical characterization of a sample in both reflected and transmitted light (back-scattered electron imaging also can be of assistance) is essential.

With prior knowledge of the matrix (*e.g.*, from EPMA), it is possible to model the depth in the sample from which X rays of interest are generated. For most practical purposes, thin sections in excess of 50 μm will stop 2–3 MeV protons; such sections can be regarded as thick targets (rather than thin, transmission, targets of finite thickness) when modeling the stopping power and excitation volume in the sample.

Other uses for proton beams

Proton beams also provide a variety of other analytical techniques applicable to mineralogical and geochemical analysis; these are (1) Nuclear Reaction Analysis (NRA; Boni *et al.* 1988, Moncoffre *et al.* 1990), (2) Proton-Induced Gamma-ray Emission (PIGE; Anderson *et al.* 1989, Tulhoat *et al.* 1993), (3) Proton Activation Analysis (PAA; Halden & Hawthorne 1993). These techniques depend upon the interaction of the proton beam with the nucleus of the atom of interest. A variety of reactions and decay schemes may be available for any particular element (depending on proton energy and reaction cross-section), and decay products such as γ rays, α particles and X rays (from electron-capture processes) may be available for detection (the number of photons or particles being, in part, a function of the abundance of the element of interest). PIGE and NRA have been used to analyze samples for Li, B, F, Mg, Al, Si and P; Tulhoat *et al.* (1993) have shown that concentrations of Li, B, F and Na can be measured in spodumene, tourmaline and lepidolite, with detection limits in the 60–100 ppm range. These techniques require detectors other than the Si(Li) detector used in energy-dispersion PIXE; depending on the design of the specimen chamber, nuclear reactions may be detected concurrently with PIXE.

Proton beams also may be used to create images *via* such processes as ion luminescence (Yang *et al.* 1993), Scanning Transmission Ion Microscopy (STIM), microtomography (Schofield & Lefèvre 1993) and ion back-scattering. The PIXE–STIM combination can be used to analyze and image an object below the surface of the sample, and it is applicable wherever the proton beam can penetrate the material being analyzed. In addition, Channeling Contrast Microscopy (CCM) can been used to determine the position of trace elements in a structure and could have value in studies of site occupancy, *e.g.*, Au in minerals such as pyrite (Jamieson & Ryan 1993).

It is clear that our understanding of minerals and their role in natural and industrial processes will develop further as we expand our range of analytical tools. Earth scientists and physicists have much to gain by cooperating in the use of this new generation of analytical instrumentation.

ACKNOWLEDGEMENTS

This work was supported by the Natural Sciences and Engineering Research Council through grants to N.M.H and J.L.C. We thank Roger Mason for use of the crystal of synthetic calcite. We thank Robert Martin, Frank Hawthorne, Gerry Czamanske and Peter Roeder for their constructive comments on an earlier version of this manuscript.

REFERENCES

ADAM, J., GREEN, T.H. & SIE, S.H. (1993): Proton microprobe determined partitioning of Rb, Sr, Ba, Y, Zr, Nb and Ta between experimentally produced amphiboles and silicate melts with variable F content. *Chem. Geol.* **109**, 29-49.

ANDERSON, A.J., CLARK, A.H., MA, XIN-PEI, PALMER, G.R., MACARTHUR, J.D. & ROEDDER, E. (1989): Proton-induced X-ray and gamma ray emission analysis of unopened fluid inclusions. *Econ. Geol.* **84**, 924-939.

ANNEGARN, H.J. & BAUMAN, S. (1990): Geological and mineralogical applications of PIXE: a review. *Nucl. Instrum. Methods Phys. Res.* **B49**, 264-270.

BLANK, H., EL GORESY, A., JANICKE, J., NOBILING, R. & TRAXEL, K. (1984): Partitioning of Zr and Nb between coexisting opaque phases in lunar rocks – determined by quantitative proton microprobe analysis. *Earth Planet. Sci. Lett.* **68**, 19-33.

BONI, C., CEREDA, E., BRAGA MARCAZZAN, G.M. & DE TOMASI, V. (1988): Prompt gamma emission excitation functions for PIGE analysis of Li, B, F, Mg, Al, Si and P in thin samples. *Nucl. Instrum. Methods Phys. Res.* **B35**, 80-86.

CABRI, L.J. (1988): Applications of proton and nuclear microprobes in ore deposit mineralogy and metallurgy. *Nucl. Instrum. Methods Phys. Res.* **B30**, 459-465.

________, CAMPBELL, J.L., LAFLAMME, J.H.G., LEIGH, R.G., MAXWELL, J.A. & SCOTT, J.D. (1985): Proton-microprobe analysis of trace elements in sulphides from some massive-sulphide ore deposits. *Can. Mineral.* **23**, 133-148.

CAHILL, T.A. (1980); Proton microprobes and particle induced X-ray analytical systems. *Annu. Rev. Nucl. Part. Sci.* **30**, 211-52.

CAMPBELL, J.L., CABRI, L.J., ROGERS, P.S.Z., TRAXEL, K. & BENJAMIN, T.M. (1986): Calibration of micro-PIXE analysis of sulphide minerals. *Nucl. Instrum. Methods Phys. Res.* **B22**, 437-441.

________ & COOKSON, J.A. (1984): PIXE analysis of thick targets. *Nucl. Instrum. Methods Phys. Res.* **B3**, 185-197.

________, MAXWELL, J.A., TEESDALE, W.J., WANG, J.-X. & CABRI, L.J. (1990): Micro-PIXE as a complement to electron probe microanalysis. *Nucl. Instrum. Methods Phys. Res.* **B44**, 347-356.

________, PERUJO, A., TEESDALE, W.J. & COOKSON, J.A. (1988): Minimum detection limits in PIXE analysis of thick targets. *Nucl. Instrum. Methods Phys. Res.* **B30**, 317-323.

________, TEESDALE, W.J. & HALDEN, N.M. (1995): Theory, practice and application of micro-PIXE analysis and element-distribution maps. *Can. Mineral.* **33**, 279-292.

CHEN, J.R., KNEIS, H., MARTIN, B., NOBILING, R., TRAXEL, K., CHAO, E.C.T. & MINKIN, J.A. (1981): Trace element analysis of bituminous coals using the Heidelberg proton microprobe. *Nucl. Instrum. Methods Phys. Res.* **181**, 151-157.

CZAMANSKE, G.K., KUNILOV, V.E., ZIENTEK, M.L., CABRI, L.C., LIKHACHEV, A.P., CALK, L.C. & OSCARSON, R.L. (1992): A proton-microprobe study of magmatic sulfide ores from the Noril'sk–Talnakh district, Siberia. *Can. Mineral.* **30**, 249-287.

________, SISSON, T.W., CAMPBELL, J.L. & TEESDALE, W.J. (1993): Micro-PIXE analysis of silicate reference standards. *Am. Mineral.* **78**, 893-903.

DUROCHER, J.J.G., HALDEN, N.M., HAWTHORNE, F.C. & MCKEE, J.S.C. (1988): PIXE and micro-PIXE analysis of minerals at $E_p = 40$ MeV. *Nucl. Instrum. Methods Phys. Res.* **B30**, 470-473.

FRASER, D.G. (1990): Applications of the high-resolution scanning proton microprobe in the Earth sciences: an overview. *Chem. Geol.* **83**, 27-37.

———, FELTHAM, D. & WHITEMAN, M. (1989): High-resolution scanning proton microprobe studies of micron-scale trace-element zoning in secondary dolomite: implications for studies of redox behaviour in dolomites. *Sed. Geol.* **65**, 223-232.

———, WATT, F., GRIME, G.W. & TAKACS, J. (1984): Direct determination of strontium enrichment on grain boundaries in a garnet lherzolite xenolith by proton microprobe analysis. *Nature* **312**, 352-354.

GREEN, T.H., SIE, S.H., RYAN, C.G. & COUSENS, D.R. (1989): Proton microprobe-determined partitioning of Nb, Ta, Zr, Sr, and Y between garnet, clinopyroxene and basaltic magma at high pressure and temperature. *Chem. Geol.* **74**, 201-216.

GRIFFIN, W.L., ASHLEY, P.M., RYAN, C.G., SIE, S.H. & SUTER, G.F. (1991): Pyrite geochemistry in the North Arm epithermal Ag–Au deposit, Queensland, Australia: a proton-microprobe study. *Can. Mineral.* **29**, 185-198.

———, JAQUES, A.L., SIE, S.H., RYAN, C.G., COUSENS, D.R. & SUTER, G.F. (1988): Conditions of diamond growth: a proton microprobe study of inclusions in West Australian diamonds. *Contrib. Mineral. Petrol.* **99**, 143-158.

———, RYAN, C.G., COUSENS, D.R., SIE, S.H. & SUTER, G.F. (1990): Application of the proton microprobe to diamond exploration and genesis. *Nucl. Instrum. Methods Phys. Res.* **B49**, 318-322.

GRIME, G.W. & DAVISON, W. (1993): The use of nuclear microprobe techniques to study the chemistry of lacustrine sediments and particles. *Nucl. Instrum. Methods Phys. Res.* **B77**, 430-435.

GUNN, J.S., HARROWFIELD, I.R., PROCTOR, C.H. & THRESHER, R.E. (1992): Electron probe microanalysis of fish otoliths – evaluation of techniques for studying age and stock discrimination. *Expl. Mar. Biol. Ecol.* **158**, 1-36.

HALDEN, N.M. (1993): High-energy proton beam analysis of geological materials. *Nucl. Instrum. Methods Phys. Res.* **B77**, 399-404.

——— & HAWTHORNE, F.C. (1993): Proton Activation Analysis (PAA): a complement to PIXE and PIGE analysis. *Int. PIXE* **3**, 73-79.

———, ———, CAMPBELL, J.L., TEESDALE, W.J., MAXWELL, J.A. & HIGUCHI, D. (1993): Chemical characterization oscillatory zoning and overgrowths in zircon using 3 MeV μ-PIXE. *Can. Mineral.* **31**, 637-647.

———, ———, DUROCHER, J.J.G., SMITH, G.S., GALLOP, D.M. & MCKEE, J.S.C. (1991): High-energy K-line PIXE spectra of Au-bearing minerals. *Am. Mineral.* **75**, 956-962.

HOROWITZ, P. & GRODZINS, L. (1975): Scanning proton-induced X-ray microspectrometry in an atmospheric environment. *Science* **189**, 795-797.

JAMIESON, D.N. & RYAN, C.G. (1993): Microprobe channelling analysis of pyrite crystals. *Nucl. Instrum. Methods Phys. Res.* **B77**, 415-421.

JOHANSSON, S.A.E. & CAMPBELL, J.L. (1988): *P.I.X.E.: a Novel Technique for Elemental Analysis.* J. Wiley & Sons, Chichester, U.K.

KULLERUD, G., STEFFEN, R.M., SIMMS, P.C. & RICKEY, F.A. (1979): Proton-induced X-ray emission (PIXE) – a new tool in geochemistry. *Chem. Geol.* **25**, 245-256.

LUCAS, M.A., HUGHES, T.C. & MCKENZIE, C.D. (1981): Proton microprobe dating of natural zircons. *Nucl. Instrum. Methods Phys. Res.* **191**, 34-38.

MACARTHUR, J.D. & MA, XIN-PEI (1991): A review of particle induced X-ray emission in geology. *Int. PIXE* **1**, 311-338.

MANDZIUK, W.S., BRISBIN, W.C. & SCOATES, R.F.J. (1989): Igneous structures in the Falcon Lake intrusive complex, southeastern Manitoba. *Can. Mineral.* **27**, 81-92.

MAXWELL, J.A., CAMPBELL, J.L. & TEESDALE, W.J. (1989): The Guelph PIXE software package. *Nucl. Instrum. Methods Phys. Res.* **B43**, 218-230.

———, LEIGH, R.G., CAMPBELL, J.L. & PAUL, H. (1984): Least-squares fitting of PIXE spectra with a digital filter treatment of the continuum. *Nucl. Instrum. Methods Phys. Res.* **B3**, 301-304.

MONCOFFRE, N., MILLARD, N., JAFFREZIC, H. & TOUSSET, J. (1990): Boron analysis of thin layers using prompt nuclear techniques. *Nucl. Instrum. Methods Phys. Res.* **B45**, 81-85.

O'REILLY, S.Y., GRIFFIN, W.L. & RYAN, C.G. (1991): Residence of trace elements in metasomatized spinel lherzolite xenoliths: a proton microprobe study. *Contrib. Mineral. Petrol.* **109**, 98-113.

PALMER, G.R., DIXIT, S.S., MACARTHUR, J.D. & SMOL, J.P. (1989): Elemental analysis of lake sediment from Sudbury, Canada, using particle-induced X-ray emission. *Sci. Tot. Env.* **88/89**, 141-156.

PEISACH, M. & PINEDA, C.A. (1990): K X-ray production from rare earths by high energy protons. *Nucl. Instrum. Methods Phys. Res.* **B49**, 10-14.

PERUJO, A., RIDDOLIS, T.J. & CAMPBELL, J.L. (1988): Design of a dedicated target chamber for PIXE microanalysis of mineral samples. *Nucl. Instrum. Methods Phys. Res.* **B30**, 280-283.

PETRUK, W. (1989): Image analysis for mineral beneficiation. *In* Image Analysis Applied to Mineral and Earth Sciences (W. Petruk, ed.). *Mineral. Assoc. Can., Short-Course Handbook* **16**, 86-89.

REED, S.J.B. (1990): Recent developments in geochemical microanalysis. *Chem. Geol.* **83**, 1-9.

ROEDER, P.L., MACARTHUR, D., MA, XIN-PEI, PALMER, G.R. & MARIANO, A.N. (1987): Cathodoluminescence and microprobe study of rare-earth elements in apatite. *Am. Mineral.* **72**, 801-811.

ROGERS, P.S.Z., DUFFY, C.J., BENJAMIN, T.M. & MAGGIORE, C.J. (1984): Geochemical applications of nuclear microprobes. *Nucl. Instrum. Methods Phys. Res.* **B3**, 671-676.

RYAN, C.G., COUSENS, D.R., SIE, S.H., GRIFFIN, W.L., SUTER, G.F. & CLAYTON, E. (1990): Quantitative PIXE microanalysis of geological material using the CSIRO proton microprobe. *Nucl. Instrum. Methods Phys. Res.* **B47**, 55-71.

SCHOFIELD, R.M.S. & LEFÈVRE, H.W. (1993): Analysis of unsectioned specimens: 2D tomographic PIXE with STIM. *Nucl. Instrum. Methods Phys. Res.* **B77**, 217-224.

SHIMIZU, N. (1990): The oscillatory trace element zoning of augite phenocrysts. *Earth-Sci. Rev.* **29**, 27-37.

TEESDALE, W.J., CAMPBELL, J.L. & HALDEN, N.M. (1993): Two-dimensional mapping of element variation in minerals using the Guelph proton microprobe. *Nucl. Instrum. Methods Phys. Res.* **B77**, 405-409.

TULHOAT, N., COUREL, P., TROCELLIER, P. & GOSSET, J. (1993): Stability and distribution of lithium and boron in minerals. *Nucl. Instrum. Methods Phys. Res.* **B77**, 436-443.

VALKOVIĆ, V., ORLIĆ, I., MAKJANIĆ, J., RENDIĆ, D., MIKALAVŽIČ, U. & BUDNAR, M. (1984): Comparison of different modes of excitation in X-ray emission spectroscopy in the detection of trace elements in coal and coal ash. *Nucl. Instrum. Methods Phys. Res.* **B4**, 127-131.

WOGELIUS, R.A., FRASER, D.G., FELTHAM, D.J. & WHITEMAN, M.I. (1992): Trace element zoning in dolomite: proton microprobe data and thermodynamic constraints on fluid compositions. *Geochim. Cosmochim. Acta* **56**, 319-334.

YANG, CHANGYI, LARSSON, N.P.O., SWIETLICKI, E., MALMQVIST, K.G., JAMIESON, D.N. & RYAN, C.G. (1993): Imaging with ionoluminescence (IL) in a nuclear microprobe. *Nucl. Instrum. Methods Phys. Res.* **B77**, 188-194.

Received August 9, 1993, revised manuscript accepted June 6, 1994.